JEM

Supplemental material

Chen et al., https://doi.org/10.1084/jem.20181155

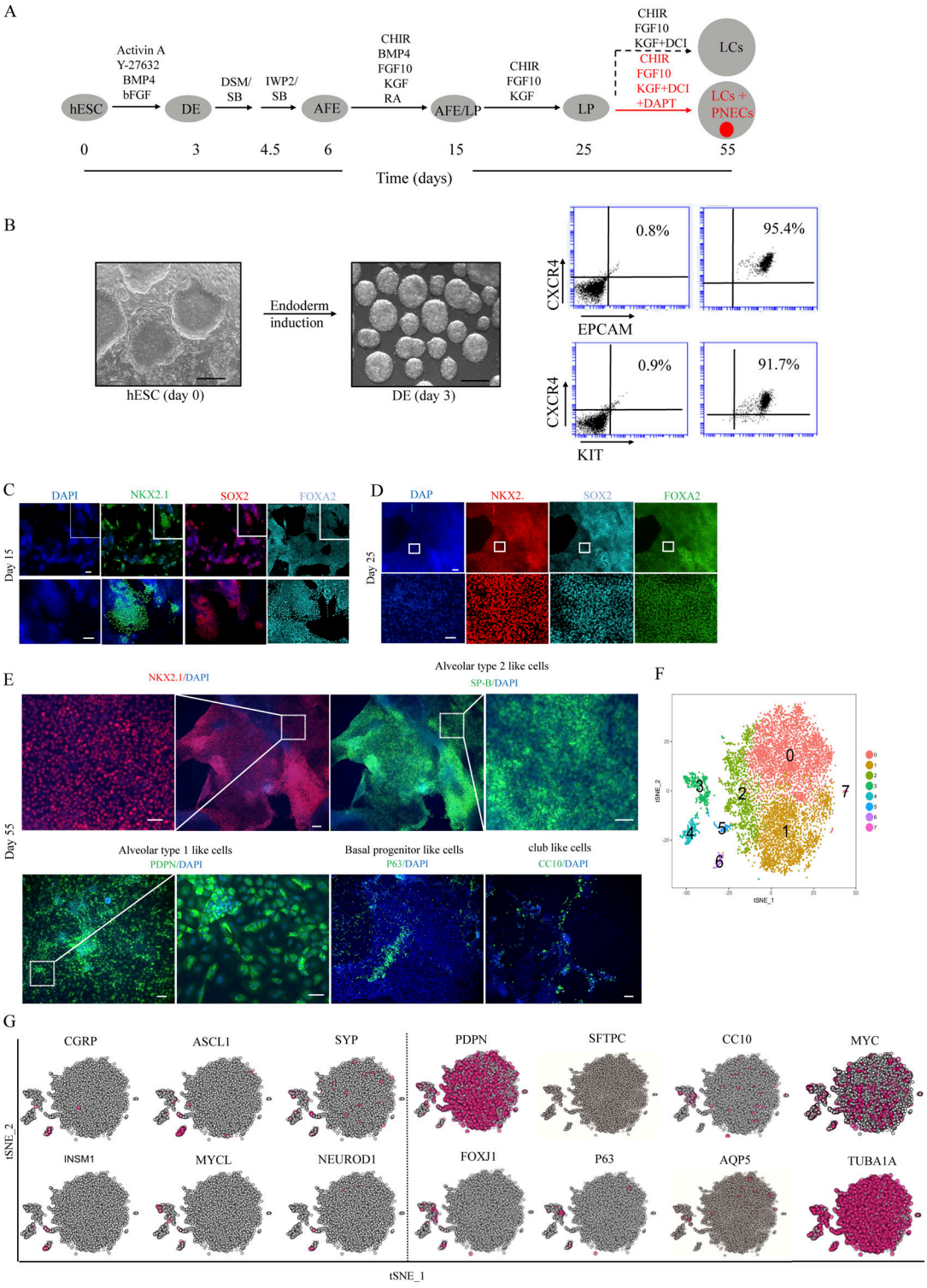

Figure S1. **Differentiation of hESCs to form DE and LCs. (A)** Similar to Fig. 1 A, but the schematic of the protocol to generate LCs from hESCs includes major components of differentiation mixtures I–VI. AFE, anterior foregut endoderm. **(B)** RUES2 cells were induced to DE, and DE cells were shown to be triply positive for CXCR4, EPCAM, and KIT by FACS with the indicated antisera (right-hand graphs). Samples stained with control IgG served as negative control (left-hand graphs). Scale bars, 0.5 mm. Endoderm was differentiated to form LP cells between day 15 (C) and day 25 (D) as shown by increasing proportions of cells positive for NKX2.1, SOX2, and FOXA2. Scale bars, 200 µm (top rows) and 50 µm (bottom rows). **(E)** Day 25 LP cells derived from hESCs (RUES2 line) were further differentiated into cells resembling major types of LCs, including AT2 (SP-B$^+$) and AT1 (PDPN$^+$) lung epithelial cells, basal progenitor cells (P63$^+$), and club cells (CC10$^+$). All were detected at day 55 by immunostaining with the indicated antisera. Biological repeats n = 5. Scale bars, 50 µm (long) and 100 µm (short). **(F)** tSNE map of scRNA profiling of day 55 LCs not exposed to DAPT, colored by cluster assignment. **(G)** Individual cells positive (red dots) for RNA corresponding to PNEC-related genes (left) and canonical markers for other LC types (right). AT1 cells, PDPN&AQP5; AT2 cells, SFTPC; club cells, CC10; ciliated cells, FOXJ1; and basal progenitor cells, P63. TUBA1A serves as internal control for gene expression during lung development. Biological repeats (n) = 2.

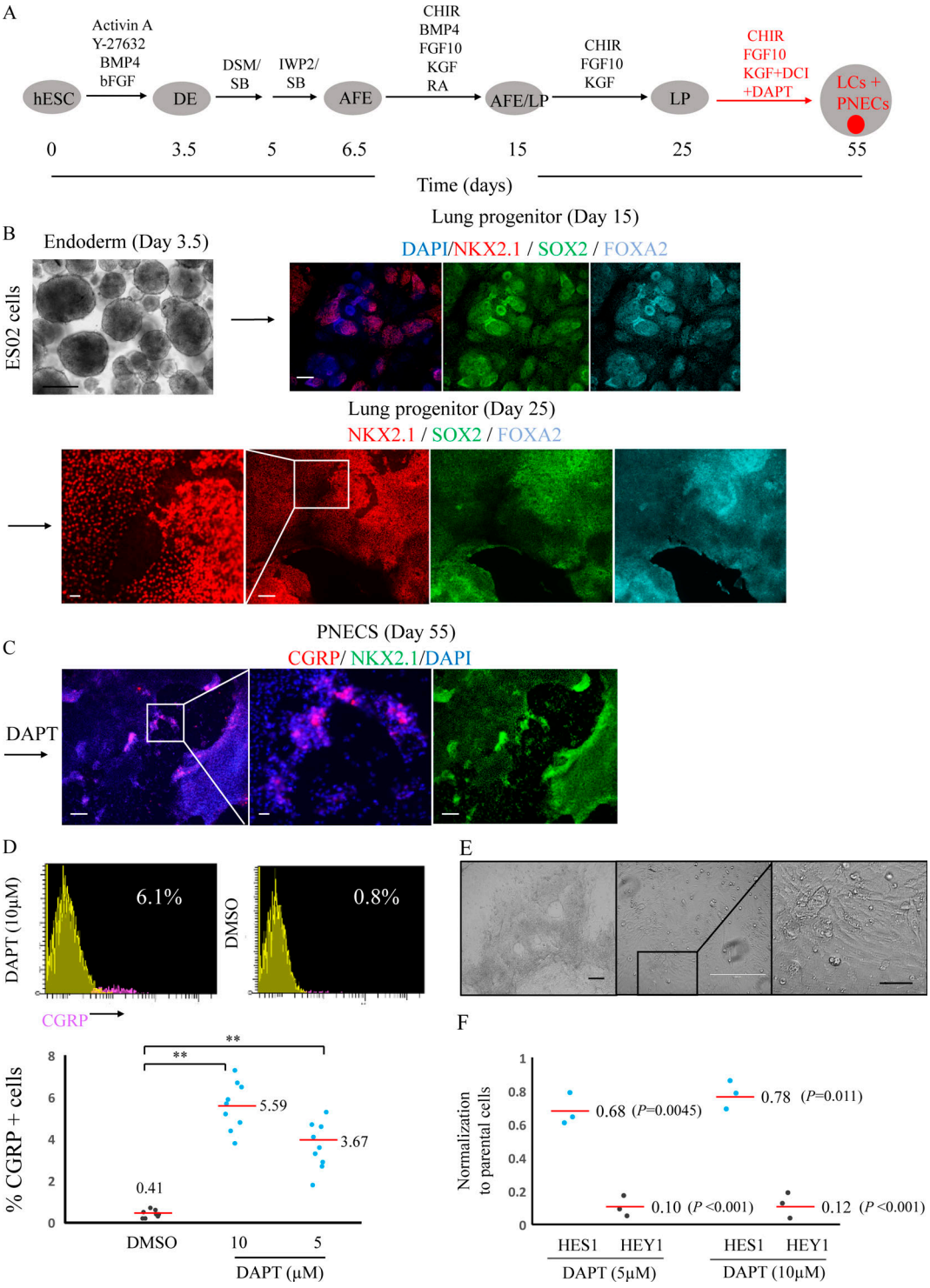

Figure S2. **DAPT induces PNECs during differentiation of the ES02 line of hESCs and gene expression after induction of PNECs with DAPT, an inhibitor of NOTCH signaling. (A)** Schematic of the protocol, as in Fig. 1 A, to generate PNECs with DAPT during differentiation of hESCs. AFE, anterior foregut endoderm. **(B)** Endoderm cells derived from the ES02 line of hESCs were further differentiated into LPs, with increasing percentages of LPs from day 15 to 25. Scale bars, 0.5 mm. **(C)** PNECs, assessed by IHC staining for CGRP, were induced by DAPT from day 25 to 55. Scale bars, 100 μm (long) and 20 μm (short). **(D)** Percentages of CGRP$^+$ cells in cultures grown with 0, 5, or 10 μM DAPT were determined at day 55 by FACS and displayed as flow cytometry data (10 μM DAPT only; red, CGRP$^+$; yellow, CGRP$^-$) and by scatter graph (bottom). **, P < 0.01 by Student's *t* test. Horizontal red lines denote average values; number of biological repeats (*n*) = 9. **(E)** Bright-field images of the RUES2 hESC-derived LCs treated with 5 μM DAPT from day 25 to 55 (left) and the fractionated culture of CGRP$^+$ cells after FACS sorting (middle and right). Scale bars, 400 μm (left and middle) and 50 μm (right). **(F)** Decreased expression of NOTCH target genes HES1 and HEY1 in day 55 LCs after exposure to DAPT from day 25 during differentiation of the RUES2 line of hESCs. Results were obtained by quantitative RT-PCR assay; the relative levels were determined by comparison with parallel tests with day 55 LCs not exposed to DAPT. P values by two-way ANOVA test. Horizontal red lines denote average values. Biological repeats (*n*) = 3.

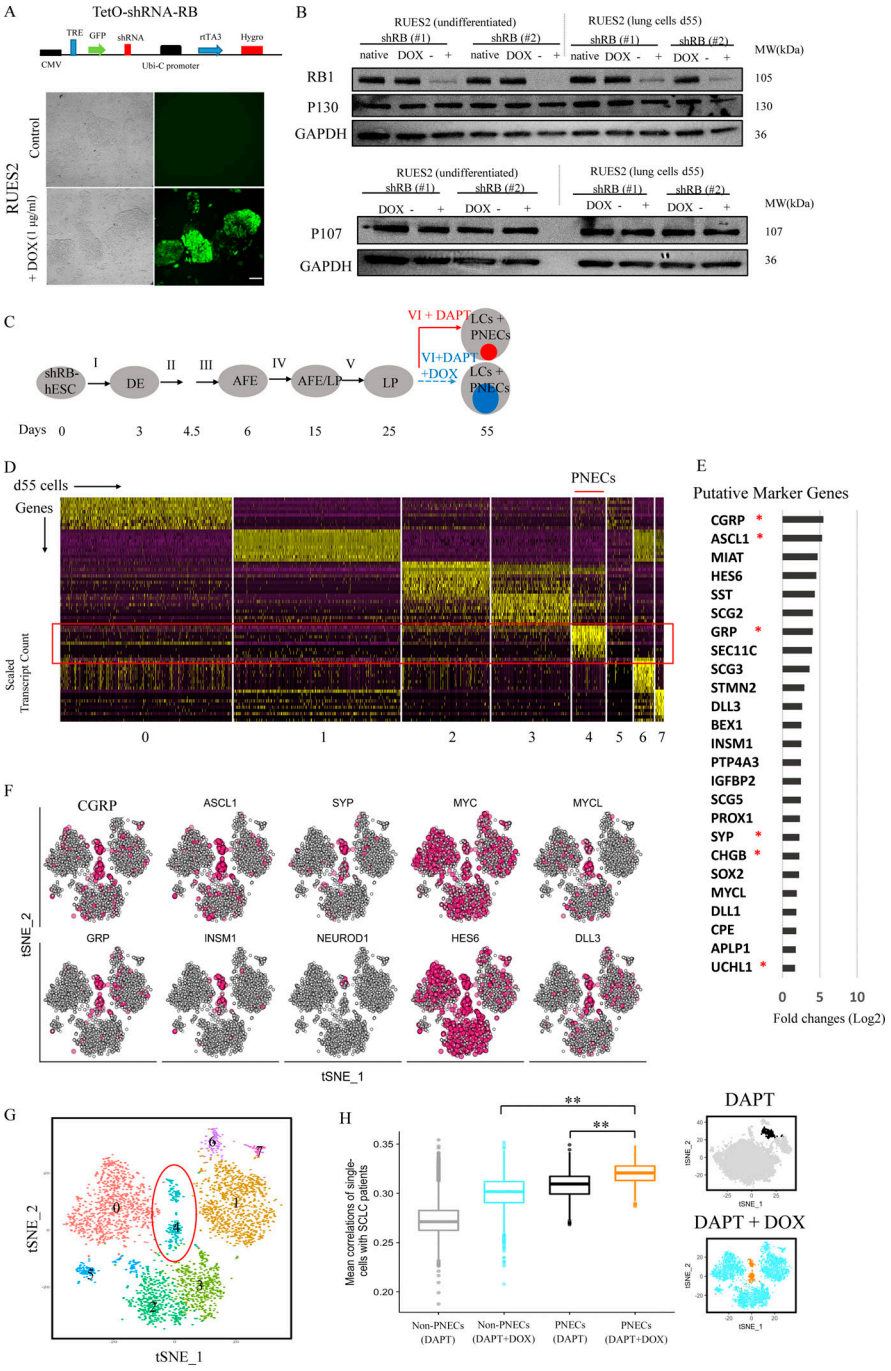

Figure S3. **Generation and characterization of PNECs through directed differentiation of hESCs in which NOTCH signaling was blocked by DAPT and RB protein levels were reduced by shRNA. (A)** Schematic of vector constructed with shRNA targeting RB (Materials and methods section) controlled by tetracycline operator (TetO; top). GFP-mediated fluorescence documents DOX-dependent expression in transgenic cells. TRE, tetracycline response element. **(B)** Reduced production of RB1 but not of RB-related proteins P130 and P107 was documented by Western blotting using the indicated antisera and extracts from undifferentiated cells and day 55 LCs derived from the transgenic RUES1 line with and without DOX treatment for 30 d. **(C)** Schematic of PNEC production from RUES2 cells carrying a DOX-inducible transgene encoding RB-specific shRNA after exposure to DAPT and DOX (as in Fig. 2 A). AFE, anterior foregut endoderm. **(D)** Single-cell RNA profiling of day 55 LCs treated with DAPT (5 μM) and DOX from day 25 to 55. Scaled expression of the most differentially expressed genes (rows) specific to different cell clusters in each cell (columns). PNEC-like cells are principally in cluster 4, but additional cells expressing some PNEC markers are found in other clusters (0, 1, 2, and 3). **(E)** PNEC markers found to be differentially expressed in the PNEC-like cell cluster. Bars indicate log fold change; asterisks indicate canonical PNEC marker. **(F)** Individual cells positive for PNEC markers and other genes associated with neuroendocrine differentiation are denoted with red dots as in Fig. 2 E. **(G)** tSNE map colored by cluster assignment as in Fig. 2 D. **(H)** PNEC and non-PNEC single-cell transcriptomes in cultures treated with DAPT alone or DAPT and DOX (to reduce RB expression) were correlated with 29 bulk RNA profiles of early-stage human SCLCs (stage 1a or 1b; George et al., 2015). The distributions of the mean correlation for each cell are presented. See text for interpretation (on the left, Spearman's Correlation, **, P < 2.2e-16, by two-sided Kolmogorov–Smirnov test). tSNE maps indicate PNEC and non-PNEC populations in cultures in which RB expression was not perturbed (top right) and cultures in which RB shRNA was induced by DOX (bottom right). Biological repeats (*n*) = 2.

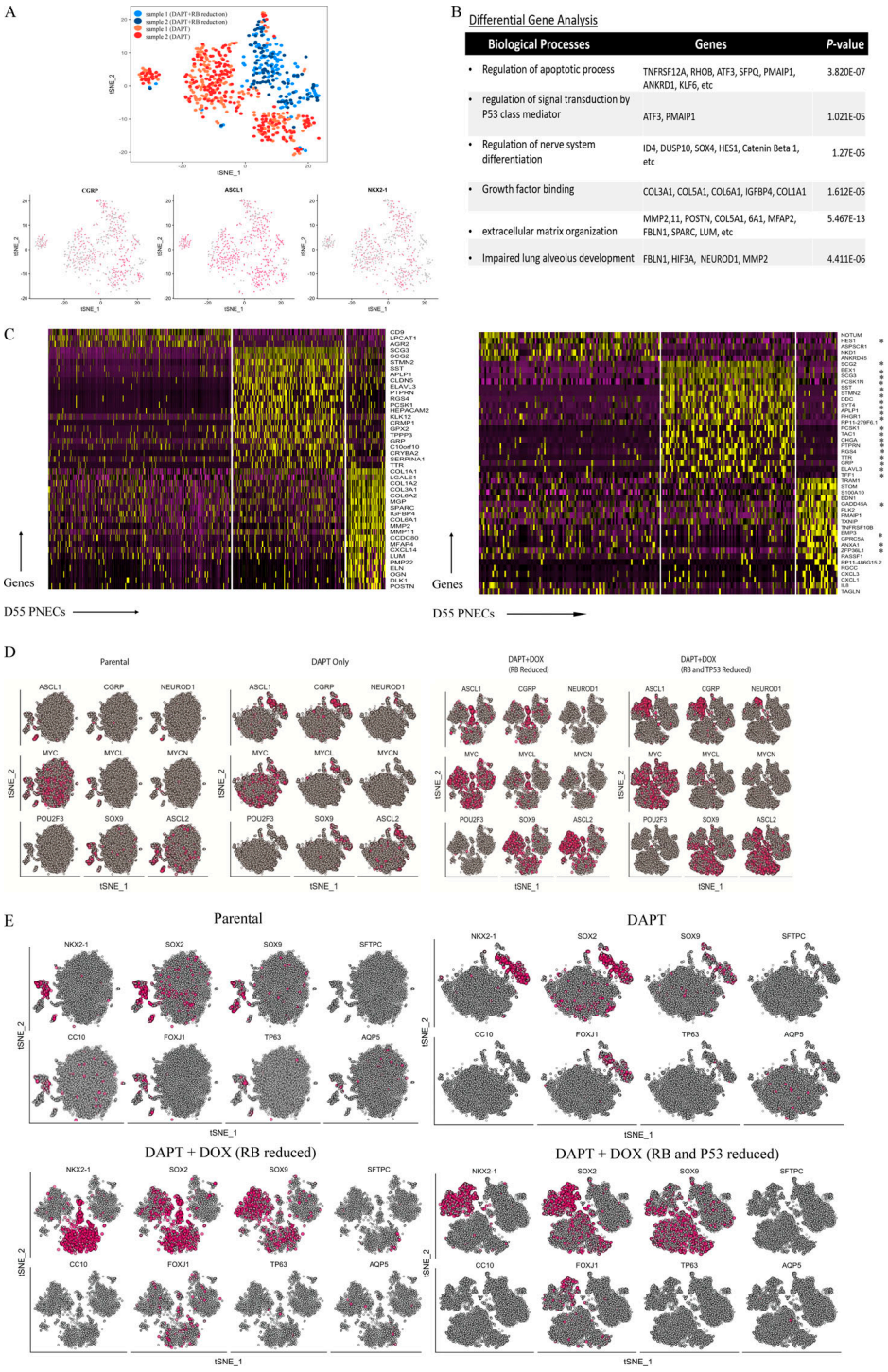

Figure S4. **Comparisons of scRNA profiles from cultures of RUES2 cells in which RB and P53 levels were and were not reduced by induction of shRNA. (A)** Reduced-dimensionality tSNE map of PNEC cells from day 55 LCs treated with DAPT (5 µM) and DOX (to reduce RB expression, blue) or with DAPT alone (red). Top: Colors denote biological replicates as listed in the key. Bottom: Individual cells positive for PNECs markers (CGRP or ASCL1) and lung lineage marker NKX2.1 are denoted by red dots. **(B)** Pathways and genes identified by Topp Gene software (Chen et al., 2009) based on differential gene expression from comparison of PNEC cells identified by scRNA profiling of cultures in which RB levels were and were not reduced. **(C)** Scaled expression of the most differentially expressed genes (rows) specific to different PNEC cell subclusters in each cell (columns). The left-hand heat map shows results with PNECs from cultures exposed to DAPT; the right-hand map shows results with PNECs from cultures exposed to DAPT, with DOX used to reduce RB levels by induction of RB shRNA. Asterisks denote the most differentially expressed genes in the subsets of PNECs treated with DAPT and DOX and are also expressed in the subsets of PNECs treated with DAPT alone. The heterogeneity within the PNEC-like cell cluster is discussed in the text. **(D)** scRNA profiling of day 55 LCs treated with DMSO (parental), DAPT (DAPT only), and with DAPT and DOX to induce shRNA targeting RB (RB reduced) or to induce shRNA targeting both RB and P53 (RB and P53 reduced) from day 25 to 55. Individual cells positive for canonical PNEC markers, other genes associated with neuroendocrine differentiation (D), and markers for other LC types (E) are denoted by red dots. Biological repeats (n) = 2.

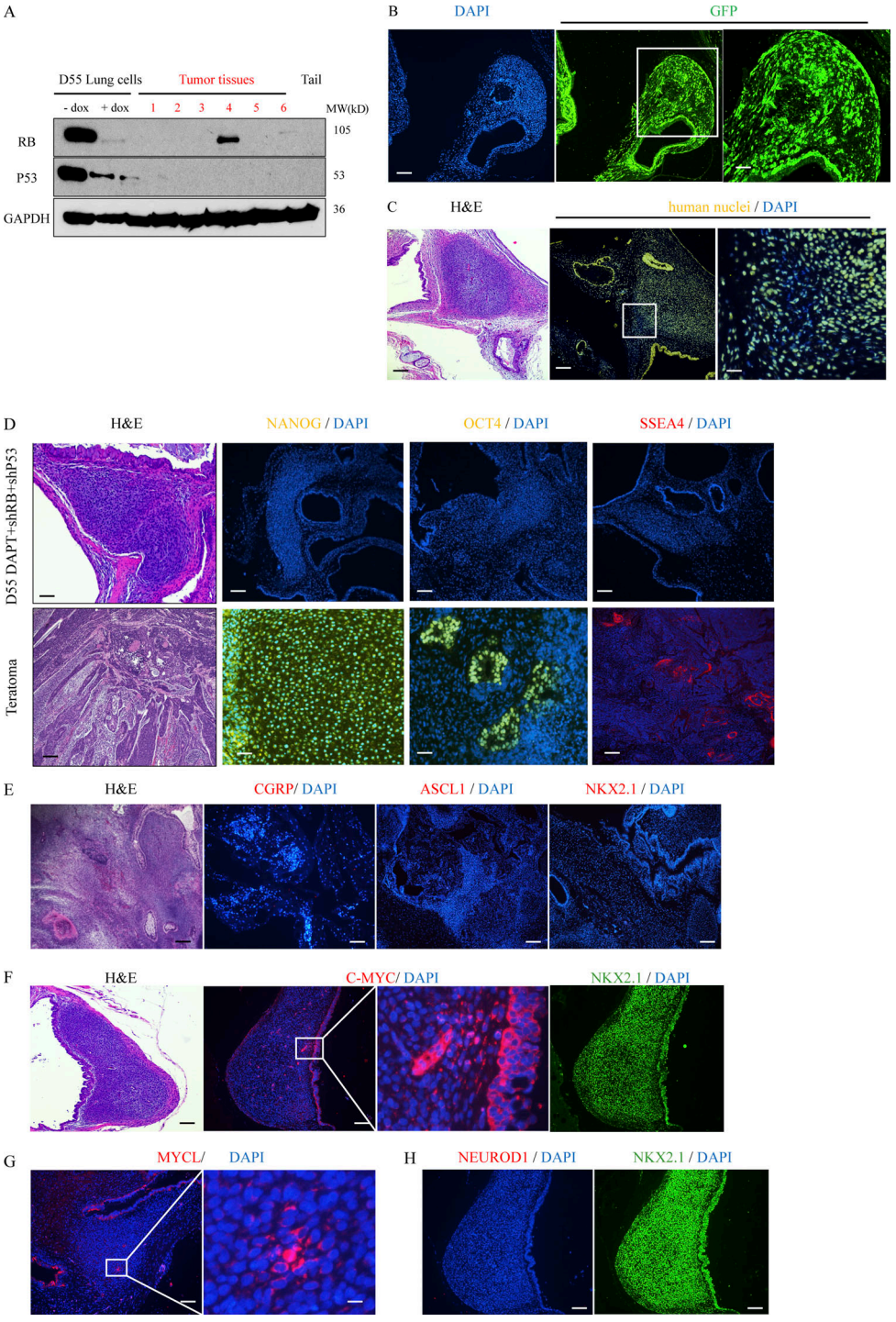

Figure S5. **Characterization of xenografts formed with hESC-derived LCs. (A–C)** DAPT-treated day 55 LCs, induced with DOX to express shRNA specific for RB1 or P53 or both, were injected subcutaneously into NSG mice. Xenografts developed after 6–7 wk only with DAPT-treated LCs in which RB and P53 were reduced by DOX induction of shRNAs. **(A)** P53 and RB proteins were measured in extracts of day 55 LCs (the first two lanes, without and with DOX treatment; six xenografts [1–6]; and a mouse tail in right-hand lane) by Western blot using antibodies against human RB or P53; GAPDH served as in internal loading control. **(B)** Origin of the tumors formed with day 55 LCs was validated by fluorescence-based detection of GFP encoded in the RB-shRNA vector. **(C)** Cells in tumor nodules formed after injection of day 55 LCs were confirmed to be of human origin by immunostaining with antibody against human nuclear-specific protein. Scale bars, 100 µm (long) and 20 µm (short). **(D–H)** Comparison of hESC-derived LC xenografts with undifferentiated hESC-derived teratomas. **(D)** Morphology of xenograft tumors formed with day 55 LCs (top left) compared with teratomas (bottom left) formed with undifferentiated RUES2 cells (H&E staining); tumors from day 55 LCs did not stain with antisera against embryonic tissue markers NANOG, OCT4, and SSEA4 (top) that were detected in tumors (teratomas; bottom) grown from undifferentiated RUES2 cells. **(E)** CGRP, ASCL1, and NKX2.1—detected in the xenograft tumors from differentiated LCs (Fig. 4)—were not detected in teratomas. Scale bars, 100 µm (long) and 20 µm (short). **(F–H)** Some cells in the xenograft tumors formed with differentiated lung calls expressed C-MYC (F) and MYCL (G) but did not express detectable amounts of NEUROD1 (H). Scale bars, 100 µm (long) and 20 µm (short). Biological repeats (n) = 3.

References

Chen, J., E.E. Bardes, B.J. Aronow, and A.G. Jegga. 2009. ToppGene Suite for gene list enrichment analysis and candidate gene prioritization. *Nucleic Acids Res.* 37:W305-11. https://doi.org/10.1093/nar/gkp427

George, J., J.S. Lim, S.J. Jang, Y. Cun, L. Ozretić, G. Kong, F. Leenders, X. Lu, L. Fernández-Cuesta, G. Bosco, et al. 2015. Comprehensive genomic profiles of small cell lung cancer. *Nature.* 524:47–53. https://doi.org/10.1038/nature14664